THE JOURNAL OF BIOLOGICAL CHEMISTRY
Vol. 277, No. 28, Issue of July 12, pp. 24870–24874, 2002

Printed in U.S.A.

Stepping Rotation of F_1-ATPase with One, Two, or Three Altered Catalytic Sites That Bind ATP Only Slowly*

Received for publication, March 18, 2002, and in revised form, April 17, 2002
Published, JBC Papers in Press, April 18, 2002, DOI 10.1074/jbc.M202582200

Takayuki Ariga‡, Tomoko Masaike‡§¶, Hiroyuki Noji‖, and Masasuke Yoshida‡§‡‡**

*From the ‡Chemical Resources Laboratory, Tokyo Institute of Technology, 4259 Nagatsuta, Yokohama, 226-8503, Japan, ‖Institute of Industrial Science, University of Tokyo, 4-6-1 Komaba, Meguro-ku, Tokyo, 153-8505, Japan, **Precursory Research for Embryonic Science and Technology, Japan Science and Technology Corporation (JST) 332-0012 and §ATP System Project, Exploratory Research for Advanced Technology, Japan Science and Technology Corporation (JST), 5800-2 Nagatsuta, Yokohama, 226-0026, Japan*

F_1-ATPase is an ATP hydrolysis-driven motor in which the γ subunit rotates in the stator cylinder $\alpha_3\beta_3$. To know the coordination of three catalytic β subunits during catalysis, hybrid F_1-ATPases, each containing one, two, or three "slow" mutant β subunits that bind ATP very slowly, were prepared, and the rotations were observed with a single molecule level. Each hybrid made one, two, or three steps per 360° revolution, respectively, at 5 μM ATP where the wild-type enzyme rotated continuously without step under the same observing conditions. The observed dwell times of the steps are explained by the slow binding rate of ATP. Except for the steps, properties of rotation, such as the torque forces exerted during rotary movement, were not significantly changed from those of the wild-type enzyme. Thus, it appears that the presence of the slow β subunit(s) does not seriously affect other normal β subunit(s) in the same F_1-ATPase molecule and that the order of sequential catalytic events is faithfully maintained even when ATP binding to one or two of the catalytic sites is retarded.

The F_oF_1-ATP synthase found in mitochondria, bacteria, and chloroplasts couples proton translocation in the F_o portion and ATP synthesis/hydrolysis in the F_1 portion through physical rotation of the central shaft subunits (1–5). The isolated F_1 portion has ATPase activity, thus often called F_1-ATPase, and is composed of five different subunits with a stoichiometry of $\alpha_3\beta_3\gamma\delta\epsilon$. The $\alpha_3\beta_3\gamma$ subcomplex is the minimum ATPase-active complex that has catalytic features similar to F_1-ATPase. In the crystal of the $\alpha_3\beta_3\gamma$ structure, α and β subunits are arranged alternately to form an $\alpha_3\beta_3$ cylinder around the coiled-coil structure of the γ subunit (6). Catalytic sites reside mainly on β subunits, whereas some residues of α subunits also contribute.

The isolated F_1-ATPase by itself is a motor enzyme; the biochemical supporting result of sophisticated subunit-exchange experiments of *Escherichia coli* F_1-ATPase (7) was secured by the direct demonstration of ATP hydrolysis-driven rotation of the fluorescent actin filament attached to the γ subunit of an $\alpha_3\beta_3\gamma$ subcomplex of thermophilic F_1-ATPase immobilized on a glass surface (8). At nanomolar ATP concentrations, the γ subunit rotates in discrete 120° steps (9). The analysis indicates that the dwell time of the step corresponds to the waiting time for the ATP molecule to occupy the next catalytic site. Further study with a smaller rotation marker and higher time resolution has revealed that a 120° step is split into a 90° substep, triggered by ATP binding, and a 30° substep, probably driven by dissociation of ADP (or phosphate) from the enzyme (10).

The mechanism of how the ATP hydrolysis drives the rotation of F_1-ATPase is intriguing. The cooperative nature of substrate binding and catalysis of F_oF_1-ATP synthase and F_1-ATPase has long been recognized and explained by a model, the binding change mechanism proposed by Boyer (11), which assumed the rotational participation of three catalytic sites during catalysis. In support of this model, three β subunits in F_1-ATPase crystals are in the three different nucleotide binding states: one β subunit with bound AMP-PNP[1] at catalytic site, another with ADP, and the third without nucleotide. The β subunits with bound nucleotides take a "closed" conformation, but the β subunit with an empty catalytic site takes an "open" conformation (6). Thus, it is likely that the rotation of the γ subunit is caused by alternative, sequential conformational transition of three β subunits in F_1-ATPase that is accompanied by each catalytic step in ATP hydrolysis. Then, the mechanism that conducts coordination of three β subunits needs to be clarified. To analyze this, the experimental system may have a great value that enables observation of the role of the individual β subunit during rotation. In this report, we describe a novel method to prepare the hybrid F_1-ATPase[2] containing one or two copies of mutant β subunit(s) that can bind ATP only slowly. Characteristic rotations of the hybrid F_1-ATPases were compared with those of wild-type F_1-ATPase

* The costs of publication of this article were defrayed in part by the payment of page charges. This article must therefore be hereby marked "*advertisement*" in accordance with 18 U.S.C. Section 1734 solely to indicate this fact.

¶ Supported by Research Fellowships of the Japan Society for the Promotion of Science for Young Scientists.

‡‡ To whom correspondence should be addressed: Chemical Resources Laboratory, R-1, Tokyo Institute of Technology, 4259 Nagatsuta, Yokohama, 226-8503, Japan. Tel.: 81-45-924-5233; Fax: 81-45-924-5277; E-mail: myoshida@res.titech.ac.jp.

[1] The abbreviations used are: AMP-PNP, adenosine 5′-(β, γ-imino) triphosphate; FEFE mutations, F414E and F420E mutations of β subunit of F_1-ATPase; F_1(0xFEFE), a mutant $\alpha(C193S)_3\beta_1\beta(His\text{-}tagged/I386C)_2\gamma(S109C/I212C)_1$ subcomplex of F_1-ATPase; F_1(1xFEFE), a mutant $\alpha(C193S)_3\beta(F414E/F420E)_1\beta(His\text{-}tagged/I386C)_2\gamma(S109C/I212C)_1$ subcomplex of F_1-ATPase; F_1(2xFEFE), a mutant $\alpha(C193S)_3\beta_1\beta(His\text{-}tagged/I386C/F414E/F420E)_2\gamma(S109C/I212C)_1$ subcomplex of F_1-ATPase; F_1(3xFEFE), a mutant $\alpha(C193S)_3\beta(His\text{-}tagged/F414E/F420E)_3\gamma(S209C/I212C)_1$ subcomplex of F_1-ATPae; MOPS, 4-morpholinepropanesulfonic acid; biotin-$PEAC_5$-maleimide, 6-N′-[2-(N-maleimido)ethyl]-N-piperazinylamidohexyl-D-biotinamide; Ni-NTA, nickel nitrilotriacetic acid; HPLC, high pressure liquid chromatography; BSA, bovine serum albumin; pN, piconewtons.

[2] Actually, an $\alpha_3\beta_3\gamma$ subcomplex of thermophilic F_1-ATPase was used for experiments in this study. However, hereafter in this report, we also call this subcomplex F_1-ATPase for simplicity unless confusion occurs.

and mutant F_1-ATPase with three mutant β subunits. The results show that the binding of ATP to one β subunit in F_1-ATPase is rate-limiting for a corresponding single 120°-step rotation in these mutants and that the sequence of catalytic events in F_1-ATPase is not confused even if one of the ATP binding steps is delayed.

EXPERIMENTAL PROCEDURES

Strains, Plasmids, and Protein Preparation—E. coli strains used were JM109 for preparation of plasmids, CJ236 for generation of uracil-containing single-stranded plasmids for site-directed mutagenesis, and JM103Δ(*uncB-uncD*) for expression of the mutant $\alpha_3\beta_3\gamma$ subcomplexes and mutant β subunits of F_1-ATPase of thermophilic *Bacillus* strain PS3. Plasmids pUC-β, which carried genes for the β subunit of thermophilic F_1-ATPase, and pKAGB1, which carried genes for the α, β, and γ subunits of thermophilic F_1-ATPase (12), were used for mutagenesis and for gene expression. The plasmid pkk-HC95 (pKAGB1/α(C193S)/γ(S109C/I212C)/β(His tag at the N terminus)) has been described previously (10). The plasmid pkk-C95 (pKAGB1/α(C193S)/γ(S109C/I212C)/β), which is a non-His-tagged version of pkk-HC95, was prepared by ligating a 7.4-kb *Nhe*I-*Pma*CI fragment of pkk-HC95 and a 1.3-kb fragment of pKAGB1. The $\alpha_3\beta_3\gamma$ subcomplexes expressed from either pkk-HC95 or pkk-C95 were considered the wild-type F_1-ATPase in this report. Plasmids pUC-β and pUC-β(I386C/His tag) containing the 1.4-kb *Mlu*I-*Pst*I fragment of the β subunit of thermophilic F_1-ATPase were used for site-directed mutagenesis to introduce "FEFE" mutations (β(F414E/F420E)) by the Kunkel method (13) with the synthetic oligonucleotide 5′-GTA CGA GCC CGG TTG *A*CC *G*GT **TTC** CTG CTC CGC CAC GTG **TTC** GTT TTG CGA CAA GAA GAA C-3′ where bold letters are changes made for the mutations Phe to Glu, and italic letters indicate silent mutations that introduce an *Age*I site used to identify the mutant. The 1.4-kb *Mlu*I-*Pst*I fragment of this plasmid containing the FEFE mutations was ligated with the 7.4-kb *Mlu*I-*Pst*I fragment of pkk-HC95 to produce pkk-HC95FEFE and that of pkk-C95 to produce pkk-C95FEFE. The final plasmids used for expression of the mutant products were proved correct by direct nucleotide sequence determination. The expressed $\alpha_3\beta_3\gamma$ subcomplex and β subunits were purified as described previously (12, 14) and were stored in 70% ammonium sulfate.

Preparation of Hybrid Complexes—It has been known that the dimer of β subunits is formed in F_1-ATPase through a disulfide bond between cysteines introduced at the position of β-Ile-386 (15). We have adopted this mutation to obtain a β dimer that can reconstitute F_1-ATPase with other subunits. The outline of the procedures to isolate F_1(1xFEFE) is as follows (see Fig. 1*A*). 1) The β(I386C/His tag) dimers were generated from monomers and isolated. The β(I386C/His tag) subunits in ammonium sulfate suspension were centrifuged and dissolved in 40 mM Tris-HCl, pH 8.0, and 100 mM NaCl. To dimerize β subunits, the solution was treated with 100 μM $CuCl_2$ for 2 h at room temperature. The solution was concentrated to 200 μl by ultrafiltration and was subjected to a gel filtration HPLC column Superdex 200HR (Amersham Biosciences) that had been equilibrated with potassium P_i buffer (0.1 M potassium phosphate, pH 7.0, 2 mM EDTA). The peak fraction of the β(I386C/His tag) dimer was collected and was applied again to the same column. 2) Two cysteines in the γ subunit of F_1(3xFEFE) were labeled with biotin-maleimide. The F_1-ATPase, containing three β(FEFE)s but not His tag, in ammonium sulfate was centrifuged, dissolved in potassium P_i buffer, and reduced with 20 mM dithiothreitol for 4 h at room temperature. The solution was subjected to a gel filtration HPLC column (Superdex 200HR, Amersham Biosciences) that had been equilibrated with potassium P_i buffer, and the protein peak fraction was treated with a 20-fold molar excess of biotin-$PEAC_5$-maleimide for 2 h at room temperature. Unbound reagents were removed with a PD-10 column (Amersham Biosciences). 3) Thus, treated F_1(3xFEFE) and β(I386C/His tag) dimers were mixed and denatured by urea. Biotinylated F_1-ATPase (0.7 mg) was thus obtained, and a 3-fold molar amount of purified β(I386C/His tag) dimers was dissolved in 1 ml of potassium P_i buffer. The proteins were denatured by the addition of 120 mg of solid urea and were incubated at 4 °C for 1 h. 4) Urea was diluted, and the proteins were concentrated. The solution was diluted with a 50-fold amount of a wash buffer (50 mM imidazole-HCl, pH 8.0, 100 mM NaCl) plus 100 μM ATP and 2 mM $MgCl_2$ and concentrated to 1 ml by ultrafiltration. By these procedures, F_1(1xFEFE) complexes were assembled from the β(FEFE) subunit, biotin-labeled γ subunit, and the β(I386C/His tag) dimer. Other molecular species were also present in the solution: assembled F_1(3xFEFE), free β(FEFE) monomer, free α subunit, free γ subunit, and free β(I386C/His tag) dimer. 5) The former four species without His tag were removed by passing through an Ni-NTA column. The solution was passed through an Ni-NTA Superflow column (1.5-ml bed volume, Qiagen) equilibrated with the wash buffer. The column was washed with 6 ml of the wash buffer and eluted with 6 ml of elution buffer (200 mM imidazole-HCl, pH 8.0, 100 mM NaCl). 6) F_1(1xFEFE) was isolated from free β(I386C/His tag) dimer by gel filtration. The eluate was concentrated to 200 μl with ultrafiltration and was subjected to a gel filtration HPLC column (Superdex 200HR, Amersham Biosciences) that had been equilibrated with potassium P_i buffer. The hybrid F_1(1xFEFE) that contained a β(I386C/His tag) dimer and a β(FEFE) subunit was eluted as an isolated protein peak separated from unassembled β(I386C/His tag) dimer. 7) The disulfide cross-link in F_1(1xFEFE) was reduced just prior to the rotation assay. To reduce the cross-link, the isolated peak fraction of F_1(1xFEFE) was treated with 100 mM dithiothreitol for 1 h at room temperature and was used for assays within a day. Similarly, F_1(2xFEFE) was obtained from the β(FEFE/I386C/His tag) dimer and the wild-type F_1-ATPase. F_1(0xFEFE) was also obtained by reconstitution from the β(I386C/His tag) dimer and the wild-type F_1-ATPase.

Rotation Assay Using Beads—The two cysteines of the γ subunit (S109C/I212C) were labeled with biotins (10, 16). To visualize the rotation of the γ subunit under a microscope, a duplex of streptavidin-coated beads (mean diameter: 330 or 530 nm, Bangs Laboratories, Inc.) was attached to the γ subunit. An observation flow cell (10 μl) was made of two KOH-cleaned or Ni-NTA-coated[3] coverslips (9). Molecules of F_1-ATPases (10 μl, 30 nM) were applied to the flow cell and incubated for 2 min at room temperature to fix them on the glass surface. Unbound molecules of F_1-ATPase were washed out with 20 μl of a BSA buffer (10 mM MOPS, pH 7.0, 50 mM KCl, 2 mM $MgCl_2$, and 10 mg/ml bovine serum albumin). The flow cell was infused with 10 μl of 0.5 weight percent streptavidin-coated beads in BSA buffer, incubated for 10 min at room temperature, and washed with 20 μl of BSA buffer to remove unbound beads. The flow cell was infused with 20 μl of 200 μM ATP buffer (BSA buffer containing 0.1 mg/ml creatine kinase, 1 mM creatine phosphate, and indicated concentrations of Mg-ATP), and rotation was observed. Then, 40 μl of 5 μM ATP buffer was infused into the flow cell, and the rotation was observed again. Finally, the solution was exchanged with 40 μl of 10 mM ATP buffer, and the rotation was observed again. These procedures of buffer exchange ensured that the stepping rotation was ATP concentration-dependent and not due to an artifact. Movement of beads was observed with a phase contrast microscope (IX70; Olympus). Observed images were collected through a charge-coupled device camera (CCD-300-RC; Dage-MTI) and recorded on a digital video tape at 30 frames/s. Analysis of rotation angle was performed as described previously (8, 9).

Measurement of Torque Force—The biotinylated F_1-ATPases were conjugated with streptavidin and were immobilized on the glass surface of the flow cell (9). The flow cell was infused with 10 μl of 1 nM fluorescent actin filament instead of beads, incubated for 10 min at room temperature, washed with 20 μl of BSA buffer, and infused with 20 μl of 5 mM ATP buffer. The fluorescent actin filament was observed with a fluorescence microscope (IX70; Olympus). Observed images were recorded with an intensified charge-coupled device camera (ICCD-350F; Videoscope) on a digital video tape. Analysis of rotational angle and computation of torque force were preformed as described previously (9).

Assay of ATPase Activity—ATPase activity was measured at 25 °C in the presence of an ATP-regenerating system (17) consisting of 300 μg/ml pyruvate kinase, 300 μg/ml lactate dehydrogenase, 2.5 mM phosphoenolpyruvate, and 0.2 mM NADH and indicated concentrations of Mg-ATP in MOPS buffer (10 mM MOPS-KCl, pH 7.0, 50 mM KCl, 2 mM $MgCl_2$). The initial hydrolysis rate was determined from the slope of absorbance decrease at 340 nm within 5 s after the initiation of the reaction.

RESULTS

FEFE Mutant—To generate mutants that can bind substrate ATP slowly, we replaced two phenylalanine residues of β subunits, Phe-414 and Phe-420, which are located at the "adenine-binding pocket" (6), with glutamic acid residues. These mutations of the β subunit are called FEFE in this report, and according to the number of copies of β(FEFE) subunits contained, we designate the mutant F_1-ATPases as F_1(0xFEFE),

[3] H. Itoh, H. Noji, M. Yoshida, and K. Kinosita, Jr., unpublished results.

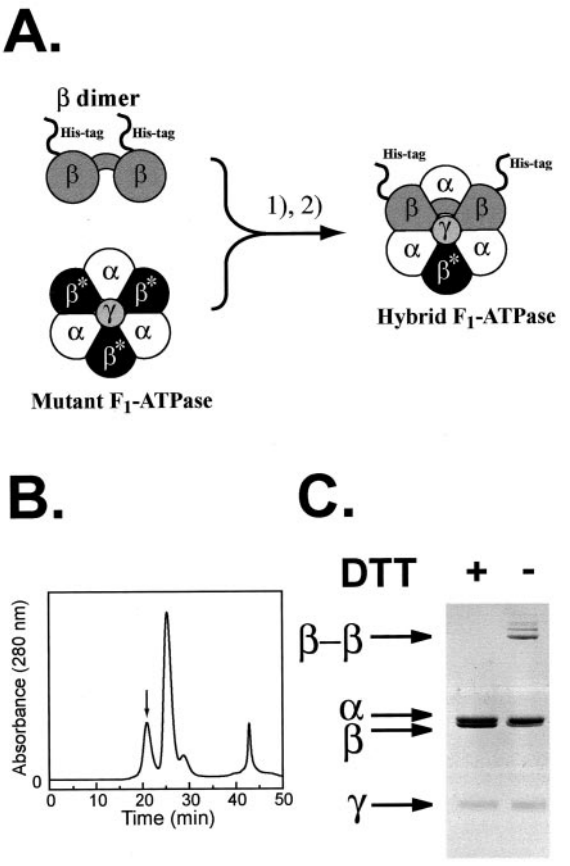

FIG. 1. **Isolation of hybrid F_1-ATPase.** *A*, the procedures to isolate hybrid complexes. *1)* The His-tagged β dimer, cross-linked between Cys-386 of two β subunits, and F_1(3xFEFE) were mixed, denatured, renatured, and reassembled. *2)* Hybrid F_1(1xFEFE) was purified with Ni-NTA and gel filtration columns. *B*, elution profile of the gel filtration HPLC monitored by absorbance at 280 nm. The His-tagged F_1(1xFEFE) was eluted at 21 min as indicated by an *arrow*. The peaks at 26 and 43 min correspond to β dimer and ATP, respectively. *C*, polyacrylamide gel electrophoresis of F_1(1xFEFE) in the presence of sodium dodecyl sulfate. The purified F_1(1xFEFE) was incubated at room temperature for 1 h (+) with or (−) without 100 mM dithiothreitol (*DTT*) and applied on the 13% gel.

TABLE I
Kinetic parameters of the mutants

F_1-ATPase	V_{max}	K_m
	turnover/sec	*mM*
F_1(0xFEFE)	71	0.016
F_1(1xFEFE)	38	0.45
F_1(2xFEFE)	85	0.90
F_1(3xFEFE)	62[a]	1.55[a]

[a] Obtained from the steady-state ATPase activity.

F_1(1xFEFE), F_1(2xFEFE), and F_1(3xFEFE).

Isolation of Hybrid F_1-ATPases—As has been described under "Experimental Procedures," F_1(1xFEFE) was isolated by gel filtration HPLC (Fig. 1*B*). The analysis of the *arrowed* peak fraction in Fig. 1*B* with non-reducing SDS-PAGE showed the bands of β dimer and β monomer with consistent band intensities (Fig. 1*C*, *right lane*). The β dimer band disappeared and the intensity of the β monomer band increased after dithiothreitol treatment (Fig. 1*C*, *left lane*). The disulfide cross-link in F_1(1xFEFE) was reduced just prior to the rotation assay. F_1(2xFEFE) and F_1(0xFEFE) were prepared by similar procedures (see "Experimental Procedures").

Bulk Phase Kinetics of the Mutants—The initial rates of ATP hydrolysis by F_1(0xFEFE), F_1(1xFEFE), and F_1(2xFEFE) were measured and analyzed by non-linear regression analysis assuming simple Michaelis-Menten kinetics (Table I). For F_1(3xFEFE), since ATP hydrolysis started with a lag phase, the steady-state rate of ATP hydrolysis, instead of the initial rate, was used for analysis. As expected, FEFE mutations resulted in the dramatic decrease of ATP affinity, and the K_m value of F_1(3xFEFE) was almost 100 times larger than that of F_1(0xFEFE). The K_m values of F_1(1xFEFE) and F_1(2xFEFE) are approximately one-third and two-third of the K_m value of F_1(3xFEFE), respectively, reflecting the occurrence of one or two times of slow ATP binding in a catalytic turnover for each mutant.[4] In contrast, the V_{max} values of the mutants remain in the same order with the value of F_1(1xFEFE) being the smallest. It should be added that the K_m value of F_1(0xFEFE) is similar to that of the wild-type F_1-ATPase (0.027 mM), whereas the V_{max} value of F_1(0xFEFE) is about 40% of that of the wild type (162 s^{-1}). The decreased V_{max} value of F_1(0xFEFE) is

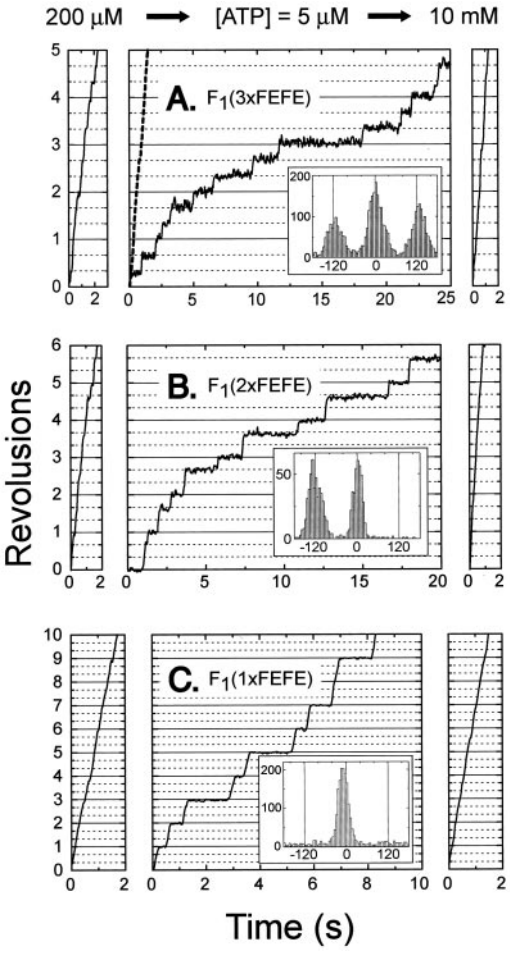

FIG. 2. **Stepping rotations of the mutant F_1-ATPases.** Time course of the rotations of the beads attached to the γ subunits of F_1(3xFEFE) (*A*), F_1(2xFEFE) (*B*), and F_1(1xFEFE) (*C*) at 200 μM ATP (*left*), 5 μM ATP (*center*), and 10 mM ATP (*right*). Rotation of the same molecule of F_1-ATPase was observed at three ATP concentrations that were changed by infusion. The *dashed line* in *panel A* is the rotation of the wild-type F_1-ATPase at 5 μM ATP. *Insets* show histograms (number of events) of the angular positions (degree) of the beads at 5 μM ATP at each frame. These histograms are taken from the rotations observed at 0–140 s (*A*), 0–66 s (*B*), and 0–30 s (*C*).

[4] Assuming that three catalytic sites have the same k_{cat} and independent, different k_{on}^{ATP} and k_{off}^{ATP}, rate of ATP hydrolysis (V) at steady-state catalysis is calculated as $V = V_{max}S / \{S + (K_m^1 + K_m^2 + K_m^3)/3\}$; S = concentration of ATP, $K_m^{1,\ 2,\ or\ 3} = (K_{off}^{ATP,\ 1,\ 2,\ or\ 3} + K_{cat})/(K_{on}^{ATP,\ 1,\ 2,\ or\ 3})$. Because K_m^{FEFE} (K_m of F_1(3xFEFE)) $\gg K_m^{wild\text{-}type}$, K_m of F_1(1xFEFE) = $(K_m^{FEFE} + K_m^{wild\text{-}type} + K_m^{wild\text{-}type})/3 = (1/3)K_m^{FEFE}$, and K_m of F_1(2xFEFE) = $(K_m^{FEFE} + K_m^{FEFE} + K_m^{wild\text{-}type})/3 = (2/3)K_m^{FEFE}$.

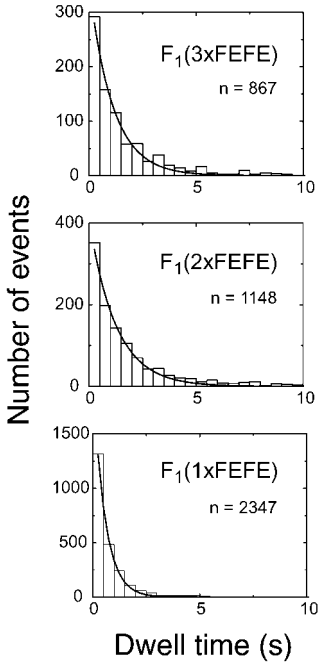

FIG. 3. **Histogram of the dwell times between steps.** All steps of all observed molecules that rotated (n = 867 for F_1(3xFEFE), 1148 for F_1(2xFEFE), 2347 for F_1(1xFEFE)) were counted. *Solid lines* show the exponential fit by the following equation. *Const* $\times$ exp($-(k_{on}^{ATP}) \times$ [ATP]t), k_{on}^{ATP} of F_1(3xFEFE) = 1.82×10^5 M^{-1} s^{-1}, k_{on}^{ATP} of F_1(2xFEFE) = 1.60×10^5 M^{-1} s^{-1}, k_{on}^{ATP} of F_1(1xFEFE) = 3.67×10^5 M^{-1} s^{-1}.

probably due to the presence of two β-I386C mutations that differentiate F_1(0xFEFE) from the wild-type F_1-ATPase. The turnover rate of F_1(1xFEFE) is about half the rates of other hybrids. The reason is not known, but possibly the prepared F_1(1xFEFE) contained more fraction in inhibited states of the enzyme than those of the other hybrids. Taken together, it is safe to conclude that FEFE is a "K_m mutation"; the effect of the FEFE mutations is predominantly restricted to the decrease of ATP binding affinity.

Stepping Rotation of Mutant F_1-ATPases—Rotation of F_1-ATPase, monitored by beads attached to the γ subunit, was observed successively at 200 μM ATP at first, at 5 μM ATP next, and then at 10 mM ATP. These procedures ensured that the observed stepping motions were not artifacts caused by, for example, surface obstacles. At 5 μM ATP, in the case of the wild-type F_1-ATPase, ATP binding should take place within 10 ms, and rotation of beads (330 or 530 nm diameter) was seen only as smooth rotation by impeding viscous friction (Fig. 2*A*, *dashed line*) (9). Similar to the wild-type F_1-ATPase, all of the 27 molecules of F_1(0xFEFE) that we observed at 5 μM ATP showed smooth rotation without steps (data not shown).

F_1(3xFEFE), on the contrary, showed the rotation with three discrete steps per revolution at 5 μM ATP (Fig. 2*A*, *solid line*). The positions of the dwells are separated from each other by about 120°, reflecting 3-fold symmetric locations where ATP binding occurs (Fig. 2*A*, *inset*). For F_1(2xFEFE), more than half of the molecules (11 out of 19) in which we detected rotation showed the rotation with two discrete steps per revolution at 5 μM ATP (Fig. 2*B*). The step positions are separated by about 120° and 240° from each other (Fig. 2*B*, *inset*). The rest of the eight molecules rotated like F_1(1xFEFE). This apparent high percentage of the molecules rotating like F_1(1xFEFE) is probably due to the unstable nature of F_1(2xFEFE); a smaller fraction of F_1(2xFEFE) might survive during the procedures of rotation assay than contaminating F_1(1xFEFE). In the case of F_1(1xFEFE), almost all rotating molecules, 34 out of 39, rotated

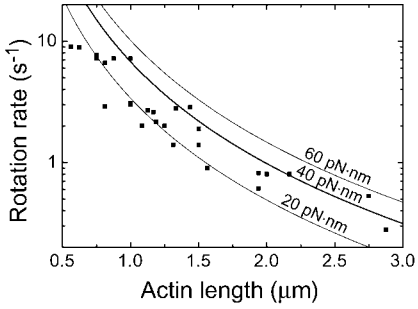

FIG. 4. **Rotational rate of F_1(3xFEFE) and length of the actin filaments.** Rotational rates in revolutions per second averaged over a continuous five revolutions are plotted *versus* the length of the actin filaments. The concentration of ATP was 5 mM. *Lines* show the theoretical rate under constant torques: 20, 40, and 60 pN·nm.

with a single step separated by 360° during revolutions at 5 μM ATP (Fig. 2*C* and *inset*). The remaining five molecules rotated like F_1(0xFEFE), that is, without step. The stepping rotations described above are all dependent on ATP concentrations. At 200 μM ATP, rotations of all mutants were rather smooth, but a rotation trajectory was slightly rugged by occasional brief steps (<0.1 s). At 10 mM ATP, all rotations were smooth and fast. It should be worth noting that even during a long dwell time, obvious single backward rotation was not observed throughout the whole experiment.

Rate Constant of ATP Binding—The dwell times at 5 μM ATP of all rotating molecules examined for F_1(3xFEFE) were collected and plotted (Fig. 3, *top*). The histogram is well fitted by a single exponential curve, suggesting that the dwell time corresponds to the waiting time of the enzyme for the next ATP and that binding of a single ATP drives one 120° rotation (9). The rate constant for ATP binding (k_{on}^{ATP}) is obtained from the fitting as 1.8×10^5 M^{-1}s^{-1}. Similar analyses were carried out for a two-step rotation of F_1(2xFEFE) and a single-step rotation of F_1(1xFEFE) (Fig. 3, *middle* and *bottom*), and k_{on}^{ATP} values of 1.6×10^5 M^{-1} s^{-1} and 3.7×10^5 M^{-1}s^{-1}, respectively, were obtained. These values of mutants were 2 orders of magnitude smaller than the k_{on}^{ATP} value of the wild type (3×10^7 M^{-1}s^{-1}) (10). As described, the K_m value of F_1(3xFEFE) is 2 orders of magnitude larger than that of F_1(0xFEFE) (and the wild-type F_1-ATPase). Therefore, the increase in K_m value of FEFE mutations can be explained solely by the decrease in the k_{on}^{ATP} value.

The fact that k_{on}^{ATP} values of F_1(1xFEFE), F_1(2xFEFE), and F_1(3xFEFE), obtained from the above analysis are similar to each other[5] implies that ATP binding to β(FEFE) in F_1-ATPase occurs at the same rate regardless of how many β(FEFE) and normal β subunits are present in the F_1-ATPase. In F_1(2xFEFE), for example, the ATP binding to the first β(FEFE) during steady-state catalysis is neither decelerated by the presence of the second β(FEFE) nor accelerated by the third normal β subunit. It seems that the effect of slow ATP binding to the first β(FEFE) is restricted to the corresponding 120° rotation driven by that ATP binding.

Torque Force of Rotation—Instead of beads, an actin filament was attached to the γ subunit, and rotation velocities

[5] The k_{on}^{ATP} value of F_1(1xFEFE) is about double of the values of other mutants. However, we do not take this difference seriously at this stage because k_{on}^{ATP} values obtained from dwell time observed for *each* of rotating molecules varied from one molecule to another. The k_{on}^{ATP} values calculated for F_1(1xFEFE), F_1(2xFEFE), and F_1(3xFEFE) are (3.4 ± 2.2) $\times 10^5$ M^{-1} s^{-1} (23 molecules), (1.2 ± 0.6) $\times 10^5$ M^{-1} s^{-1} (8 molecules), and (1.8 ± 0.8) $\times 10^5$ M^{-1} s^{-1} (8 molecules), respectively. The reason for this scattering is not known, but it may arise from either molecular individuality or uncontrolled difference of experimental conditions.

were measured for F_1(3xFEFE) at 5 mM ATP. As shown in Fig. 4, the rotational velocities decreased as the length of the actin filament increased. The observed rotations were scattered mostly between two theoretical lines that assumed the constant torque forces, 20 and 40 pN·nm. Higher velocities are thought to be more reliable because any obstructions against rotation would reduce the velocity. Therefore, we conclude that F_1(3xFEFE), similar to the wild-type F_1-ATPase, exerted constant torque of ~40 pN·nm (9).

DISSCUSSION

F_1-ATPase Does Not Easily Confuse the Order of Catalytic Sequence—This study reports that when one, two, or three β subunits in F_1-ATPase become slow in binding of substrate ATP, an obvious consequence is the retardation of initiating one, two, or three 120° rotations. During a long period in which one slow β subunit waits for ATP, other β subunits are also just waiting without letting the next catalytic event start. The principle underlying this seemingly natural consequence is the faithfulness of F_1-ATPase in keeping the order of sequential catalytic events. Also confirmed is the assumption that although three catalytic sites exist in F_1-ATPase, catalytic events of all three sites are coordinated essentially as a single, linear chain reaction pathway, excluding possibilities of other diverging-converging or parallel reaction pathways. This is another expression of Boyer's binding change mechanism, and this report provides a support for it from the rotation kinetics. Previously, we reported that when one of the β subunits in F_1-ATPase was replaced with an incompetent β subunit, catalytic turnover of ATP hydrolysis was completely blocked (14). Two other active β subunits cannot exert their catalytic ability until a preceding catalytic event, which is impossible for the incompetent β subunit, finishes.

Probably related to the above contention is the absence of the backward step during prolonged dwell time. Previously, occasional backward steps, about once per 20 forward steps, were observed and were supposed to be caused by the ATP binding to the wrong empty catalytic site (9). If so, under the situation in which the next correct ATP binding site is on the β(FEFE) subunit and the wrong binding site is on the normal β subunit, chances for the wrong site to bind ATP (and thus cause a backward step) should have increased drastically because ATP binding to the correct site is retarded about 100 times. However, such frequent backward steps were not observed for F_1(1xFEFE) and F_1(2xFEFE), and therefore, ATP binding to the wrong site does not account for the backward steps. The above argument is based on the bi-site catalysis model (18–20) in which two catalytic sites are empty at the moment just before a new ATP binds to the enzyme. If the tri-site catalysis is assumed (21–24), only one catalytic site is available for the next ATP binding and wrong ATP binding cannot occur. In this context, faithful order of catalysis of F_1-ATPase revealed in this study is explained more easily by the tri-site model than the bi-site model.

Energy of ATP Binding and Torque—It has been known that a 120°-step rotation is composed of 90- and 30°-substep rotations (10). The 90°-substep rotation is likely driven by the energy liberated when F_1-ATPase binds (but not hydrolyzes) ATP, and subsequent 30°-substep rotation occurs in ~2 ms. The method employed here did not resolve the substeps, and we observed a 120°-step rotation triggered by ATP binding. The magnitude of energy to be liberated upon ATP binding varies depending on the binding affinity of ATP to F_1-ATPase. Then k_{on}^{ATP} values of β(FEFE) in F_1-ATPase mutants are 2 orders of magnitude smaller than the wild type, and therefore, the affinity of ATP to the mutants is also very low. Nonetheless, the observed torque force of F_1(3xFEFE) is not significantly changed from that of the wild-type F_1-ATPase. In the converse combination of catalytic site and substrate, that is, when wild-type F_1-ATPase binds GTP or ITP, whose binding affinity was lower than ATP, the observed torque forces were not significantly changed from those observed for ATP (25). These apparent contradictions are explained by the "binding zipper" model proposed by Oster *et al.* (26, 27). In this model, the process of ATP binding to F_1-ATPase is divided into two subprocesses: the docking of ATP and zipping of hydrogen bonds between phosphate moiety of ATP and residues of the catalytic site. The torque force is not generated at the docking process but during the zipping process. The FEFE mutations contain mutations at the adenine-binding pocket rather than at the phosphate binding residues in F_1-ATPase. It is plausible that this mutation might reduce the chance for the docking of ATP (or the chance to enter the zipping process), but once the ATP-binding mode can transit into the zipping process by chance, the same torque force is exerted.

Acknowledgments—We thank M. Kotaka for actin preparation. We also thank Drs. T. Suzuki, E. Muneyuki, H. Itoh, T. Nishizaka, Y. Yasuda, K. Adachi, and K. Kinosita, Jr. for critical discussion.

REFERENCES

1. Mitchell, P. (1961) *Nature* **191,** 144–148
2. Boyer, P. D. (2000) *Biochim. Biophys. Acta* **1458,** 252–262
3. Weber, J., and Senior, A. E. (2000) *Biochim. Biophys. Acta* **1458,** 300–309
4. Cross, R. L. (2000) *Biochim. Biophys. Acta* **1458,** 270–275
5. Ren, H., and Allison, W. S. (2000) *Biochim. Biophys. Acta* **1458,** 221–233
6. Abrahams, J. P., Leslie, A. G. W., Lutter, R., and Walker, J. E. (1994) *Nature* **370,** 621–628
7. Duncan, T. M., Bulygin, V. V., Zhou, Y., Hutcheon, M. L., and Cross, R. L. (1995) *Proc. Natl. Acad. Sci. U. S. A.* **92,** 10964–10968
8. Noji, H., Yasuda, R., Yoshida, M., and Kinosita, K., Jr. (1997) *Nature* **386**, 299–302
9. Yasuda, R., Noji, H., Kinosita, K., Jr., and Yoshida, M. (1998) *Cell* **93**, 1117–1124
10. Yasuda, R., Noji, H., Yoshida, M., Kinosita, K., Jr., and Itoh, H. (2001) *Nature* **410**, 898–904
11. Boyer, P. D. (1993) *Biochim. Biophys. Acta* **1140,** 215–250
12. Matsui, T., and Yoshida, M. (1995) *Biochim. Biophys. Acta* **1231,** 139–146
13. Kunkel, T. A., Bebenek, K., and McClary, J. (1991) *Methods Enzymol.* **204,** 125–139
14. Amano, T., Hisabori, T., Muneyuki, E., and Yoshida, M. (1996) *J. Biol. Chem.* **271,** 18128–18133
15. Tsunoda, S. P., Muneyuki, E., Amano, T., Yoshida, M., and Noji, H. (1999) *J. Biol. Chem.* **274,** 5701–5706
16. Hirono-Hara, Y., Noji, H., Nishiura, M., Muneyuki, E., Hara, K. Y., Yasuda, R., Kinosita, K., Jr., and Yoshida, M. (2001) *Proc. Natl. Acad. Sci. U. S. A.* **98**, 13649–13654
17. Kato, Y., Sasayama, T., Muneyuki, E., and Yoshida, M. (1995) *Biochim. Biophys. Acta* **1231,** 275–281
18. Milgrom, Y. M., Murataliev, M. B., and Boyer, P. D. (1998) *Biochem. J.* **330,** 1037–1043
19. Boyer, P. D. (2002) *FEBS Lett.* **512,** 29–32
20. Kinosita, K., Jr., Yasuda, R., Noji, H., and Adachi, K. (2000) *Philos. Trans. R. Soc. Lond. B Biol. Sci.* **355,** 473–489
21. Weber, J., and Senior, A. E. (2001) *J. Biol. Chem.* **276,** 35422–35428
22. Ren, H., and Allison, W. S. (2000) *J. Biol. Chem.* **275,** 10057–10063
23. Menz, R. I., Walker, J. E., and Leslie, A. G. W. (2001) *Cell* **106,** 331–341
24. Yoshida, M., Muneyuki, E., and Hisabori, T. (2001) *Nat. Rev.* **2,** 669–677
25. Noji, H., Bald, D., Yasuda, R., Itoh, H., Yoshida, M., and Kinosita, K., Jr. (2001) *J. Biol. Chem.* **276**, 25480–25486
26. Oster, G., and Wang, H. (2000) *J. Bioenerg. Biomembr.* **32,** 459–469
27. Oster, G., and Wang, H. (2000) *Biochim. Biophys. Acta* **1458,** 482–510